Clin Neuroradiol (2015) 25:161–171
DOI 10.1007/s00062-014-0293-7

ORIGINAL ARTICLE

Posterior Reversible Encephalopathy Syndrome: The Spectrum of MR Imaging Patterns

O. Kastrup · M. Schlamann · C. Moenninghoff · M. Forsting · S. Goericke

Received: 8 April 2013 / Accepted: 17 January 2014 / Published online: 20 February 2014

Abstract
Aim The aim of this study was to describe lesion patterns, distribution, and evolution in posterior reversible encephalopathy syndrome (PRES) in a larger single-center population.
Methods Scans and follow-up, if available, of 50 patients with PRES between 2002 and 2011 were reviewed retrospectively. Lesion patterns, extent, and signal intensity changes were identified and graded on fluid-attenuated inversion recovery (FLAIR) and diffusion-weighted images. Hemorrhagic changes were identified on T2* or susceptibility-weighted images, and gadolinium enhancement on T1-weighted images was identified if available.
Results The most frequently affected regions on FLAIR were the frontal lobes in 54 %, occipital lobes in 34.3 %, and parietal lobes in 31.0 % of cases, thus 65.3 % in the posterior regions. Temporal lobes were affected in 10.6 %, the cerebellum in 6.5 %, and basal ganglia in 1.6 %. Division into vascular supply showed involvement in the anterior circulation in 66.5 % and in the posterior circulation in 33.5 % of cases. On diffusion-weighted imaging (DWI), vasogenic edema was observed in 6.9 %, cytotoxic edema in 9.1 %, and both in 2 % of cases. In 31.9 %, there was shine through, and in 15.9 %, there was shine through as well as cytotoxic or vasogenic edema. Topologic distribution on DWI showed affection of the frontal lobes in 43.5 %, occipital lobes in 25.8 %, parietal lobes in 17.7 %, temporal lobes in 11.3 %, and cerebellum in 1.6 %. T2* or susceptibility-weighted images showed spot-like hemosiderin accumulation in 17.2 % of cases. In 23.1 %, enhancement was seen. Follow-up magnetic resonance imaging showed complete resolution in 66.6 % of patients.
Conclusion The spectrum of imaging findings in PRES is wide. Almost always subcortical and cortical structures are involved. Although posterior changes are prominent in this syndrome, frontal involvement is more frequent than posterior on FLAIR imaging and DWI. On DWI, mixed patterns are not uncommon. Reversibility generally takes place independent of DWI pathology. Hypertension was not a prognostic factor.

Keywords PRES · Imaging pattern · Posterior · Leukoencephalopathy · Diffusion-weighted imaging

Introduction

Posterior reversible encephalopathy syndrome (PRES) is clinically characterized by altered mental status, seizures, and often visual disturbances [1, 2]. Predisposing factors are hypertension and eclampsia, toxic triggers like immunosuppressants, classically cyclosporine or tacrolimus [3–6], chemotherapeutic agents [7], electrolyte disturbance (hypocalcemia, hypomagnesemia) [8], and various substances like tumor necrosis factor antagonists, granulocyte colony-stimu-

Electronic supplementary material: The online version of this chapter (doi: 10.1007/s00062-014-0293-7) contains supplementary material, which is available to authorized users.

O. Kastrup, MD, PhD (✉)
Department of Neurology, University of Essen, Hufelandstr. 55, 45122 Essen, Germany
e-mail: oliver.kastrup@uni-due.de

M. Schlamann, MD, PhD · C. Moenninghoff, MD · M. Forsting · S. Goericke, MD
Institute of Diagnostic and Interventional Radiology and Neuroradiology, University of Essen, Hufelandstr. 55, 45122 Essen, Germany

lating factors, and monoclonal antibodies [9, 10]. Reversible posterior changes on neuroimaging are a hallmark feature [2, 11]. Original reports described a typical neuroradiological picture of bioccipital edema on computed tomography and magnetic resonance imaging (MRI), later demonstrated in larger series [11]. The current wider definition of the syndrome and systematic description of predisposing factors were made by Hinchey et al. [11] in 1996 by introducing the term reversible posterior leukoencephalopathy (RPLS). Due to the imaging findings, the terms posterior-occipital syndrome, reversible posterior edema syndrome, RPLS, and most commonly PRES have been coined and are in use. However, single cases and small series have indicated that the lesions are by no means restricted to the white matter [12]. Contrary to the present terminology, several reports have recently pointed to the involvement of other brain regions, including frontal or temporal changes [13–15], but the exact frequency of these findings merits further investigation. With the advent of diffusion-weighted imaging (DWI), a distinction between vasogenic and cytotoxic edema became possible [16]. Many authors have stressed the importance of DWI, but it seems by no means clear whether DWI pathology is a frequent and uniform phenomenon and whether it has prognostic implications [17]. Contrast enhancement and hemorrhage have been noted [14]. Thus, the aim of the current study was to further describe lesion patterns and distribution in PRES on fluid-attenuated inversion recovery (FLAIR) images, presence of hemorrhagic changes, contrast enhancement, and findings on DWI in a larger single-center patient population as well as evolution on follow-up.

Material and Methods

The MRI of 50 patients diagnosed as PRES in our center between 2002 and 2011 were reviewed as consensus reads by two examiners (S. Goericke and O. Kastrup). The study was conducted under the ethics committee of University Duisburg-Essen. Diagnostic criteria were an acute encephalopathic picture, seizures, mental changes or focal signs, and biochemical and radiologic exclusion of other identifiable vascular or infectious diseases. Age, sex, clinical signs, and underlying conditions were identified. MRI was performed in all cases in the first 48 h after symptom onset, and follow-up at variable intervals. All scans were done on Siemens 1.5-T scanners (Symphony, Sonata, Espree, Avanto) with FLAIR [repetition time (TR): 9,000 ms, echo time (TE): 105 ms, slice thickness (Sl): 6 mm], T1 after contrast ($n=39$, TR: 500 ms, TE: 12 ms, Sl: 6 mm), T2* ($n=20$, TR: 795 ms, TE: 26 ms, Sl: 6 mm), or later susceptibility-weighted imaging (SWI; $n=9$, TR: 49 ms, TE: 40 ms, Sl: 2 mm) sequences. Lesion patterns were identified on FLAIR images, and their distribution in anatomical regions and vascular territories was noted. The anatomical division was made in frontal, parietal, occipital, and temporal lobes as well as in basal ganglia and cerebellar location; the vascular division was subdivided into anterior and posterior circulation. The vascular allocation of frontal, parietal, and temporal lobes as well as basal ganglia was considered to belong to the anterior circulation, and the vascular allocation of the occipital lobe as well as cerebellum and brainstem to the posterior circulation. The extent of lesions was visually graded quantitatively into small, moderate, and widespread. Hyperintensity of lesions was graded as faint or bright. If available, hemorrhagic changes were identified on T2* or SWI images. Signal changes on DWI were identified on b1000 images and apparent diffusion coefficient (ADC) maps. Lesion size was graded as on FLAIR images, and hyperintensity was graded into faint or bright. Gadolinium enhancement on T1-weighted images was identified if available.

Results

Fifty patients were identified (27 female and 23 male). Age range was 4–70 (mean: 27.7 years, median: 21.5 years). Mean arterial pressure at symptom onset was < 105 mmHg (normotensive) in 20 (60.6%), 106–115 mmHg (mildly hypertensive) in 5 (15.1%), and > 115 mmHg (severely hypertensive) in 8 cases (24.2%). Subdivision into age-groups showed normotension in 70% of patients younger than 16 years and severe hypertension in 30%. In those older than 16 years, there was normotension in 23.1%, mild hypertension in 23.1%, and severe hypertension in 53.8%. A total of 37 patients had elevated C-reactive protein, 10 were febrile with intercurrent infection, and two were septic.

Underlying conditions are given in detail in Table 1, which also provides a detailed overview of clinical data, regional lesion distribution and extent, signal appearance on FLAIR and DWI, contrast enhancement findings on T2*/SWI and DWI, as well as appearance on FLAIR in the available follow-up. Analysis of MRI lesion pattern on FLAIR images disclosed that of 50 patients, 8 (16%) had involvement of one brain region only; among these, only 3 patients (6%) had isolated involvement of the occipital lobes, 4 had involvement of the parietal lobes, and 1 had isolated bitemporal involvement. In all, 10 patients (20%) had involvement of two, 14 (28%) had of three, 8 (16%) had of four, and 4 (8%) had of five regions (Fig. 1). The distribution of lesions was mainly symmetrical: 71% of all lesions were symmetric with small, moderate, and widespread extent, and 29% of all lesions were unilateral. A total of 27 patients (54%) showed exclusively symmetric pattern in one to five brain regions, 18 (36%) showed mixed symmetric and asymmetric distribution, and 5 (10%) had unilateral lesions in one to four brain regions.

Table 1 Patients' characteristics and findings on initial MRI (FLAIR and DWI 1) and on follow-up (FLAIR 2). FU (d) denotes the days until follow-up

Pat. No.	Sex	Age [ys.]	Clinical features	FLAIR (1)					T2* (1)	SWI (1)	T1+Gd (1)	DWI (1)					FLAIR (2)	
													b1000		ADC Map		evaluation	FU [d]	evaluation
					right	left	Intensity	c/s					right	left	right	left			
1	f	16	GN, ANV, GM, AMC	F	++	++	f	c/s	n	#	#	F					st	12	CR
				P	+	++	f					P							
				T		++	f					T		↑		↑			
				O		++	f					O		↑		↑			
2	f	22	E, GM, AMC	F		+	b	c/s	#	#	#	F	n	n	n	n	n	60	minimal gliosis P, O
				P	+	+	b					P							
				T								T							
				O	+	+	b					O							
				BG	+	+	b					BG							
3	m	15	histiocytosis, CSA, GM, AMC	F	+++	++	b	c/s	spot like P R	#	n	F	↑	↑	↑		mve	*	*
				P	+++	+++	b					P	↑	↑	↑↑	↑↑			
				T	+		b					T			↑				
				O	+		b					O			↑				
4	f	18	CS, E, GM, AMC	F				c/s	#	#	#	F	#	#	#	#	#	60	CR
				P	+	+	b					P							
				T								T							
				O								O							
5	f	19	SLE, IS, GM, AMC	F	++	++	b	c/s	n	#	#	F	n	n	↑↑	↑↑	ve	21	CR
				P	+	+	b					P			↑↑	↑↑			
				T	++	+	b					T							
				O	++	+	b					O			↑↑	↑↑			
				C	++	++	b					C			↑↑	↑↑			
6	m	8	NTX, IS, GM, AMC	F				c/s	n	#	n	F	n	n	n	n	n	*	*
				P	+		b					P							
				T								T							
				O								O							
7	f	70	herpes zoster, adeno CA, CTX, AMC	F				c/s	#	#	#	F	n	n	n	n	n	*	*
				P								P							
				T								T							
				O	++	++	f					O							
8	f	60	respiratory failure, FSHD, AMC	F	++	++	b	c/s	n	#	n	F	↑	↑	↑↑	↑↑	mve	11	regression
				P	++	++	b					P			↑↑	↑↑			
				T								T							
				O	++	++	b					O			↑↑	↑↑			
9	f	14	AML, CTX, GM, AMC	F	++	++	f	c/s	P R	#	n	F	n	n	n	n	n	90	residual P R+L, T R
				P	+		f					P							
				T								T							
				O	++	++	f					O							
10	m	9	BMT, ALL, GM, AMC	F	+++	+++	b	c/s	n	#	diffuse patchy	F			↑↑↑	↑↑↑	mve	90	CR
				P	+++	+++	b					P	↑	↑	↑↑↑	↑↑↑			
				T	++	++	b					T			↑↑	↑↑			
				O	+++	+++	b					O	↑↑	↑↑	↑↑↑	↑↑↑			
11	f	8	CSA, GM, AMC, LTX, VD	F		+	b	c/s	n	#	n	F	n	n	n	n	n	*	*
				P								P							
				T	+	+	f					T							
				O		+	f					O							
12	m	4	NTX, CSA, GM, AMC, VD	F				c/s	#	#	n	F	n	n	n	n	n	90	CR
				P		+	f					P							
				T								T							
				O								O							
				C		++	f					C							
13	m	17	ANV, GM, VD	F	+++	+++	b	c/s	#	#	cortical F, O R+L	F	↑↑	↑↑	↑	↑	st	30	regression
				P								P							
				T	+		b					T	↑	↑	↑	↑			
				O	+	+++	b					O	↑	↑	↑	↑			
14	m	8	LTX, NTX, GM, AMC	F				c/s	#	#	n	F					ce	150	CR
				P	+	++	b					P	spot ↑	spot ↑	spot ↓	spot ↓			
				T								T							
				O	+	+	b					O							
15	m	13	lymphoma, CTX, GM, AMC, VD	F	+	+	f	c/s	n	#	n	F	n	n	n	n	n	60	increase T R+L, O L
				P	++	++	f					P							
				T								T							
				O								O							
16	f	12	vasculitis, uremia, GM, AMC	F				c/s	n	#	n	F	n	n	n	n	n	60	CR
				P	+	+	f					P							
				T								T							
				O		+	f					O							
17	f	68	AML, uremia, GM, AMC	F				c/s	n	#	n	F	n	n			ve	30	minimal residual
				P	++	+	f					P				↑			
				T								T							
				O	++	++	f					O							
18	f	61	CML, CTX, focal seizures, AMC	F	+	++	b	c/s	#	#	spot like F R	F	↑		↑		mce	*	*
				P	++	++	b					P		↑	↓	↑			
				T								T							
				O	+++	++	b					O	↑	↑	↓	↑			
19	m	23	BMT, GM, AMC, VD	F	++	++	b	c/s	n	#	#	F	↑	↑	↑↑	↑↑	st	14	CR
				P	+++	+++	b					P							
				T	+++	+++	b					T	↑	↑	↑↑	↑↑			
				O	+++	+++	b					O	↑	↑	↑↑	↑↑			
				C	++	++	f					C							
20	m	28	BMT, GM, AMC	F				c/s	#	#	n	F					ce	30	CR
				P								P							
				T	+	+	f					T							
				O								O	↑		↓				

Table 1 (continued)

Pat. No.	Sex	Age [ys.]	Clinical features	FLAIR (1)					T2* (1)	SWI (1)	T1+Gd (1)	DWI (1)					FLAIR (2)	
												b1000		ADC Map		evaluation	FU [d]	evaluation
					right	left	Intensity	c/s				right	left	right	left			
21	f	22	HUS, HIV, GM, AMC	F				c/s	n	#	n	F						
				P	++	++	b					P	↑		↑	↑		
				T								T						
				O	+++	+++	b					O						
22	m	12	ANV, GM, AMC	F	+++	+++	f	c/s	#	#	diffuse patchy	F						
				P	++	++	f					P						
				T	+	+	f					T					st	*
				O	++	++	f					O						
				C	+++	+++	f					C	↑	↑	↑↑	↑↑		
23	f	44	NTX, CSA, GM, AMC	F	++	++	b	c/s	#	n	spot like F, P, T, O	F	↑	↑	↑	↑		
				P	++	++	b					P			↑	↑		
				T								T					mve	*
				O	++	++	b					O			↑	↑		
				C	+		b					C			↑	↑		
24	m	9	drug ingestion, GM, AMC	F	+++	+++	b	c/s	#	#	spot like F L	F	↑	↑	↑ + ↓	↑		
				P	++	++	b					P			↑↑	↑↑		
				T								T					mve + ce	*
				O	++	++	b					O			↑	↑		
25	f	65	VD	F				c/s	n	#	n	F		↑	↑			
				P	+	+	f					P						
				T								T					st	*
				O	+	+	f					O						
26	f	34	liver cirrhosis, polytoxicomania GM, AMC	F	+	+	f	c/s	n	#	n	F						
				P	+	+	f					P	#	#	#	#	#	*
				T								T						
				O	+	+	f					O						
27	m	46	HIV, uremia, GM, AMC	F	+	+	f	c/s	#	#	n	F						
				P	+++	+++	f					P	#	#	#	#	#	1440
				T		++	f					T						
				O		++	f					O						
28	m	11	BMT, GM, VD, AMC	F	++	++	b	c/s	n	#	n	F		↑				
				P	++	++	b					P		↑	↑	↑	st	60
				T								T						
				O		+	f					O						
29	f	33	E, CS, AMC, VD	F	++	++	b	c/s	#	#	n	F	↑	↑	↑ + spot ↓	↑		
				P	+++	+++	b					P						
				T		+	f					T					mce	*
				O	++	++	b					O						
30	m	42	CML, CTX, GM, AMC	F	+	+	f	c/s	#	#	n	F	↑		↑			
				P	+	+	f					P						
				T	+	+	f					T					st	30
				O	+	+	f					O						
31	m	18	HUS, GM, VD	F	+	++	b	c/s	#	#	n	F	↑	↑	↑	↑		
				P	+	+	b					P						
				T	+	+	b					T					st	30
				O	+	+	b					O						
32	m	20	CSA, ANV, GM, AMC	F				c/s	n	#	#	F						
				P								P						
				T								T					ve	90
				O	+	+	f					O						
				C	++	++	f					C			↑	↑		
33	f	35	E, CS, GM, VD	F				c/s	n	#	n	F						
				P	++	++	b					P	n	n	n	n	n	*
				T								T						
				O	+	+	f					O						
34	m	36	LTX, GM, VD	F	++	+	b	c/s	#	n	n	F	↑	↑	↓	↓		
				P		++	b					P	↑	↑	↓	↓		
				T								T					ce	*
				O		++	f					O						
				C		+	f					C						
35	f	42	SCT, myeloma, CTX, GM	F				s	#	#	#	F						
				P	+	+	b					P	↑	↑	↓	↓	ce	*
				T								T						
				O	+	+	b					O						
36	f	25	VD, SLE, hypertension	F				c/s	n	#	#	F						
				P								P						
				T								T					st	12
				O	+	+	b					O	↑	↑	↑	↑		regression
37	f	37	E, GM	F	+	+	f	c/s	#	#	n	F						
				P	+	+	f					P	n	n	n	n	n	21
				T								T						
				O		++	f					O						
38	f	16	E, GM	F	++	++	b	c/s	#	#	n	F	↑	↑				
				P	++	++	b					P						
				T	++	++	b					T	↑↑↑	↑	↑		st	*
				O	+	+	b					O	↑↑↑	↑	↑			
				BG	+	+	b					BG			↑			
39	m	39	SCT, GM, AMC	F	+++	+++	b	c/s	#	n	n	F	↑↑	↑↑	spot ↓ + ↑↑	↑↑↑		
				P	+++	+++	b					P					mce	*
				T								T						
				O	+++	+++	b					O						
40	f	19	SCT, M.Hodgkin, GM, AMC	F	++	++	b	c/s	#	spot like P L	spot like cortical F, P, O R+L	F						
				P	+++	+++	b					P	n	n	n	n	n	*
				T								T						
				O	+	+	f					O						

Table 1 (continued)

Pat. No.	Sex	Age [ys.]	Clinical features	FLAIR (1)					T2* (1)	SWI (1)	T1+Gd (1)	DWI (1)					FLAIR (2)	
												b1000		ADC Map		evaluation	FU [d]	evaluation
					right	left	Intensity	c/s				right	left	right	left			
41	m	24	uremia, coma, GM, AMC	F	+		f	c/s	#	spot like O R	spot-like P R							
				P	+	+	f					n	n	n	n	n	*	*
				T	+		f											
				O														
42	f	66	bronchial CA, CTX, GM, AMC	F	++	++	f	c/s	#	n	n							
				P	+	+	b					n	n	n	n	n	90	CR
				T														
				O	+	+	f											
43	f	21	hypertension, CS, GM, AMC	F	+++	+++	b	c/s	n	#	#	spot ↑	spot ↑					
				P	+++	+++	b											
				T												st	*	*
				O	+++	+	b					↑		↑↑↑				
				C	++	++	f					↑						
44	f	30	APS, pregnancy, GM, AMC	F				c/s	#	#	#							
				P	++	++	b					#	#	#	#	#	*	*
				T														
				O	+	+	f											
45	f	11	CML, CTX, VD	F				c/s	#	spot like P R+L, spot like O R	n							
				P	+	+	f					n	n	n	n	n	30	residual gliosis
				T	+	+	b											
				O	+++	+++	b											
46	f	8	ALL, CTX, GM, AMC	F				c/s	#	#	n							
				P	+	+	f					n	n	n	n	n	*	*
				T														
				O														
47	m	6	ALL, mycosis, GM, AMC	F				c/s	#	n	n							
				P	+	+	f											
				T												st	7	CR
				O									↑		↑			
48	m	13	BMT, GM, AMC	F	+	+	b	c/s	#	n	n	↑	↑	↑				
				P		++	b											
				T		+	f									st	*	*
				O	+	++	f											
49	f	61	CTX, GM, AMC	F				c/s	#	#	n							
				P	++	++	b					#	#	#	#	#	*	*
				T														
				O	++	++	b											
50	m	48	CTX, coma, GM, AMC	F				s	#	#	lepto-meningeal O R+L							
				P								#	#	#	#	#	14	CR
				T														
				O	+++	+++	b											

AMC Acute mental changes, *ARF* Acute renal failure, *APLS* Antiphospholipid antibody syndrome, *BMT* Bone marrow transplantation, *CA* Cancer, *CML* Chronic myeloid leukemia, *CS* Cesaerian section, *CSA* Cyclosporine A therapy, *CTX* Chemotherapy, *E* Eclampsia, *FSHD* Facioscapulohumeral muscular dystrophy, *GM* Grand mal seizure, *GN* Glomerulonephritis, *HIV* Human immunodeficiency virus infection, *HUS* Hemolytic uremic syndrome, *IS* Immunsuppression, *LTX* Liver transplant, *NTX* Kidney transplant, *RTX* Radiotherapy, *SCT* Stem cell transplantation, *SLE* Systemic lupus erythematosus, *VD* Visual disturbances, *s* Subcortical, # Not done, * Not available, *F* Frontal, *T* Temporal, *P* Parietal, *O* Occipital, *BG* Basal ganglia, *C* Cerebellar, *R* Right, *L* Left, *f* Faint, *b* Bright, ↑ Hyperintense, ↓ Hypointense, *CR* Complete resolution, *n* Normal, *ce* Cytotoxic edema, *mce* Mixed shine through and cytotoxic edema, *mve* Mixed shine through and vasogenic edema, *st* Shine through, *ve* Vasogenic edema

The topologic distribution and extent of lesion pathology on FLAIR are presented in Tables 2 and 3. Additional differentiation into vascular territories on FLAIR imaging showed affected regions in 66.5% of patients in the anterior and 33.5% in the posterior circulation. The extent of lesions in the anterior vs. the posterior circulation was small in 67.9 vs. 32.1%, moderate in 64.6 vs. 35.4%, and widespread in 67.4 vs. 32.6% of affected regions (supplementary information Fig. 7). DWI was available in 44 cases (88%). b1000 and ADC maps were normal in 17 (38.6%) and 15 cases (34.2%), respectively. DWI showed affected regions in 74.2% of patients in the anterior and 25.8% in the posterior circulation. ADC mapping showed affected regions in 69.9% of patients in the anterior and 30.1% in the posterior circulation. Tables 2 and 3 present DWI topologic lesion distribution and percentage of types of DWI pathology.

T2* or SWI images were available in 29 cases. In total, 24 were normal (82.8%), but 5 (17.2%) showed spot-like hemosiderin accumulation. A total of 33% (3 of 9) of SWI, but only 10% of T2* (2 of 20), images showed pathologic findings.

T1-weighted images after gadolinium enhancement were available in 39 cases. In 30 (76.9%), there was no enhancement. In nine (23.1%), enhancement was seen, which was limited/spot-like in six cases (15.4%) and diffuse/widespread in two (5.1%). One case (2.5%) showed focal occipital leptomeningeal enhancement, superficially above the brain surface. Magnetic resonance angiography (MRA) was normal in four cases.

Follow-up MRI was available in 27 cases, performed within the first 4 weeks in 14 cases, up to 3 months in six cases, up to 5 months in six cases, and after 4 years in one case. Lesion resolution was variable from the first

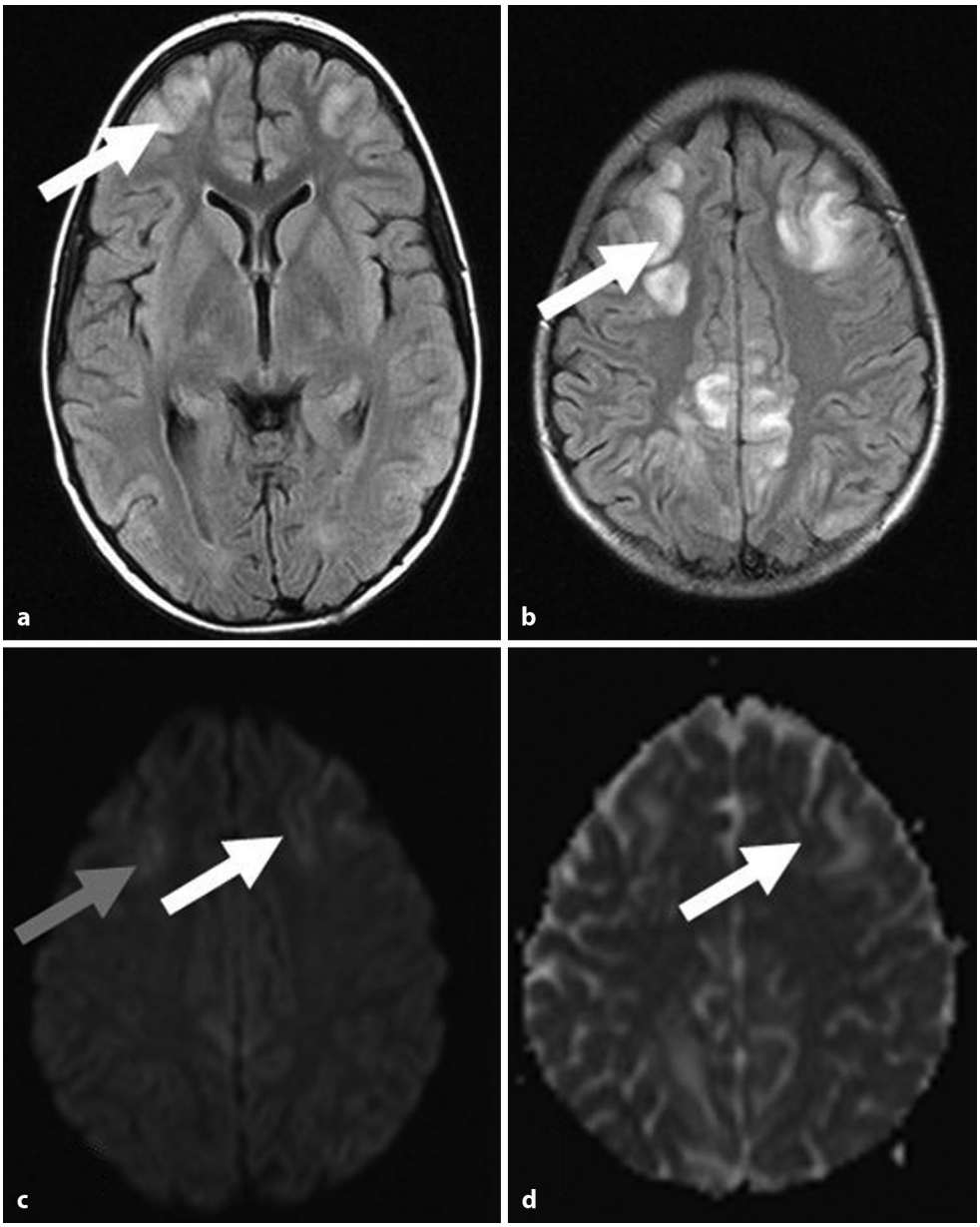

Fig. 1 Typical distribution of sub-/cortical hyperintensities in frontal (**a**) and fronto-parietal regions (**b**) on fluid-attenuated inversion recovery and diffusion-weighted imaging with hyperintensity on b1000 (**c**) and hyper-/hypointensity (shine through and cytotoxic edema) on apparent diffusion coefficient maps (**d**)

week onward. There was regression in all cases, with some patients reaching complete resolution in 1 or 2 weeks and others experiencing widespread regression in up to 1 month. A total of 18 cases (66.6%) showed complete lesion resolution. Two patients showed minimal gliotic residue at 1 and 3 months, respectively. Three patients showed regression of lesion at 2 weeks ($n=2$) and 1 month ($n=1$). In one case, there were new lesions appearing in the temporal and occipital lobes and cerebellum at 2 months, with new microhemorrhages at 3 months not visible on the acute and subacute scans (Fig. 3). One other patient showed full regression but microbleeds at 2 months. Subanalysis into hypertensive and nonhypertensive patients revealed that 23 patients showed elevated blood pressure values at symptom onset, and 27 patients were initially normotensive. Follow-up MRI was available for 13 hypertensive and 14 normotensive patients. Complete resolution of lesions in follow-up MRI was seen in 69.2 vs. 71.4% and regression with residual findings in 30.8 vs. 21.4% of patients. In one normotensive patient (7.1%), an increase in lesion numbers was found, and another showed complete resolution of lesions in FLAIR, but new microbleeds (supplementary information Fig. 8).

Analysis of DWI-positive patients with vasogenic and/or cytotoxic edema showed complete resolution in four of five (80%) cases and almost complete resolution in one. Of these patients, one showed the aforementioned microbleeds without parenchymal FLAIR signal changes. Two of two patients (100%) with purely cytotoxic edema and two of

Table 2 Topologic distribution on FLAIR and DWI

	FLAIR topology (%)	DWI topology (%)	
		b1000	ADC
Frontal	54.0	43.5	31.5
Parietal	31.0	17.7	27.0
Occipital	34.3	25.8	25.8
Temporal	10.6	11.3	10.1
Cerebellar	6.5	1.6	4.5
Basal ganglia	1.6	0.0	1.1

Table 3 Extent of MR pathology on FLAIR and DWI and types of DWI pathology

	FLAIR pathology (%)		DWI pathology (%)	
Distribution	c/sc	96.0	ve	6.9
	Pure sc	4.0	ce	9.1
Signal intensity	Bright	60.0	st	31.9
	Faint	40.0	st + ve	9.1
Expansion	Limited	32.0	st + ce	6.8
	Moderate	42.0	ve + ce	2.0
	Widespread	26.0		

c cortical, *sc* subcortical, *ve* vasogenic edema, *ce* cytotoxic edema, *st* shine through

three patients (66.6 %) with vasogenic edema showed complete resolution. Two patients with mixed patterns were available for follow-up and showed complete resolution in one and marked regression in the other case (Table 1).

Discussion

The aim of the present study was to describe the neuroimaging features of PRES in a larger population and to identify whether uniform and specific changes can be seen.

The analysis of MRI lesions on FLAIR imaging shows that posterior changes are present in two-thirds (65.3 %) of all patients. These are not solely occipital (34.3 %), but extend into the parietal lobes almost in an identical frequency (31 %). Only 6 % of cases showed isolated occipital lesions. There was a high rate of frontal involvement (54 %; Fig. 1), an aspect that was formerly considered atypical [14, 18], but has been highlighted in a recent series of 33 patients [19]. Our series demonstrates that basal ganglia involvement is rare (1.6 %), but cerebellar involvement (6.5 %) can be found more frequently than reported. Temporal changes mostly occurred together with parieto-occipital changes (Fig. 2). Almost all patients had involvement of several brain areas (3–5 discrete regions in 60 %). Involvement of only one region occurred in isolated cases only. Our additional analysis of topologic distribution into vascular territories demonstrates that in our group, the vast majority of lesions, i.e., approximately two-thirds, were found in the anterior circulation and one-third in the posterior circulation. This is in keeping with previous reports of 22 patients, with PRES showing an even higher involvement of anterior circulation structures in 91 % of cases [17]. Subanalysis into hyper- and normotensive patients demonstrated that in our cohort, those younger or older than 16 years with or without hypertension did not differ in terms of the pattern of distribution. Posterior regions are said to be more frequently involved because of less adrenoceptor supply and sympathetic innervation of the posterior circulation, making it more vulnerable to abrupt rise in blood pressure, failure of autoregulation, and blood–brain barrier disruption [20]. Our analysis of FLAIR and DWI thus does not support this theory as a single pertinent explanation. Signal intensity changes and extension of lesions on FLAIR images were variable without any specific pattern. Except for two, all cases (96 %) had affection of cortical and subcortical structures. This implies that the term leukoencephalopathy does not always apply.

The pathophysiology of PRES is not fully understood to date. Two main hypotheses have been put forward: a vasogenic and a cytotoxic mechanism. The vasogenic hypothesis assumes that excessive blood pressure overcomes cerebral autoregulation with ensuing cerebral vasodilatation and vasogenic edema [1–4, 21–26]. The cytotoxic hypothesis refers to a sudden rise in blood pressure or direct toxic mechanisms leading to cerebral vasoconstriction and formation of cytotoxic edema [18, 22, 27, 28]. Indeed, many conditions predisposing to PRES are characterized by hypertension and fluid retention, like eclampsia [27, 29]. It has been proposed that a clear differentiation between vasogenic and cytotoxic edema is crucial, as management relies on these findings. Some authors even have proposed to divide patients as having either a “hypertensive” or a “toxic” form [28, 30].

Our results of DWI imply that heterogeneous findings must be expected (Fig. 2). b1000 and ADC maps were completely normal in 38.6 % and 34.2 % of cases, respectively. In 31.9 %, there was shine-through effect; in 6.9 %, there was vasogenic edema; and in 9.1 %, there was cytotoxic edema. In 17.9 %, there were mixed hyperintense and hypointense pathologies, indicating a mixture of either shine through and vasogenic or cytotoxic edema (supplementary information Fig. 5). Also, the topology of DWI lesion distribution was noteworthy. Frontal regions were most prominently involved, followed by occipital and parietal regions on b1000 and ADC. Only few larger series have reported on the topology of DWI [14]. Earlier studies on quantitative assessment of diffusion abnormalities in PRES have postulated that vasogenic edema is more severe in the posterior white matter [31], a finding we could not replicate. These findings mandate against the hypothesis of simple vasogenic edema as the usual pathophysiology of PRES. This implies that the mechanisms of PRES are not uniform (i.e., blood–brain barrier disruption) and represent a combination of metabolic–ischemic changes. DWI does not seem to be a valid

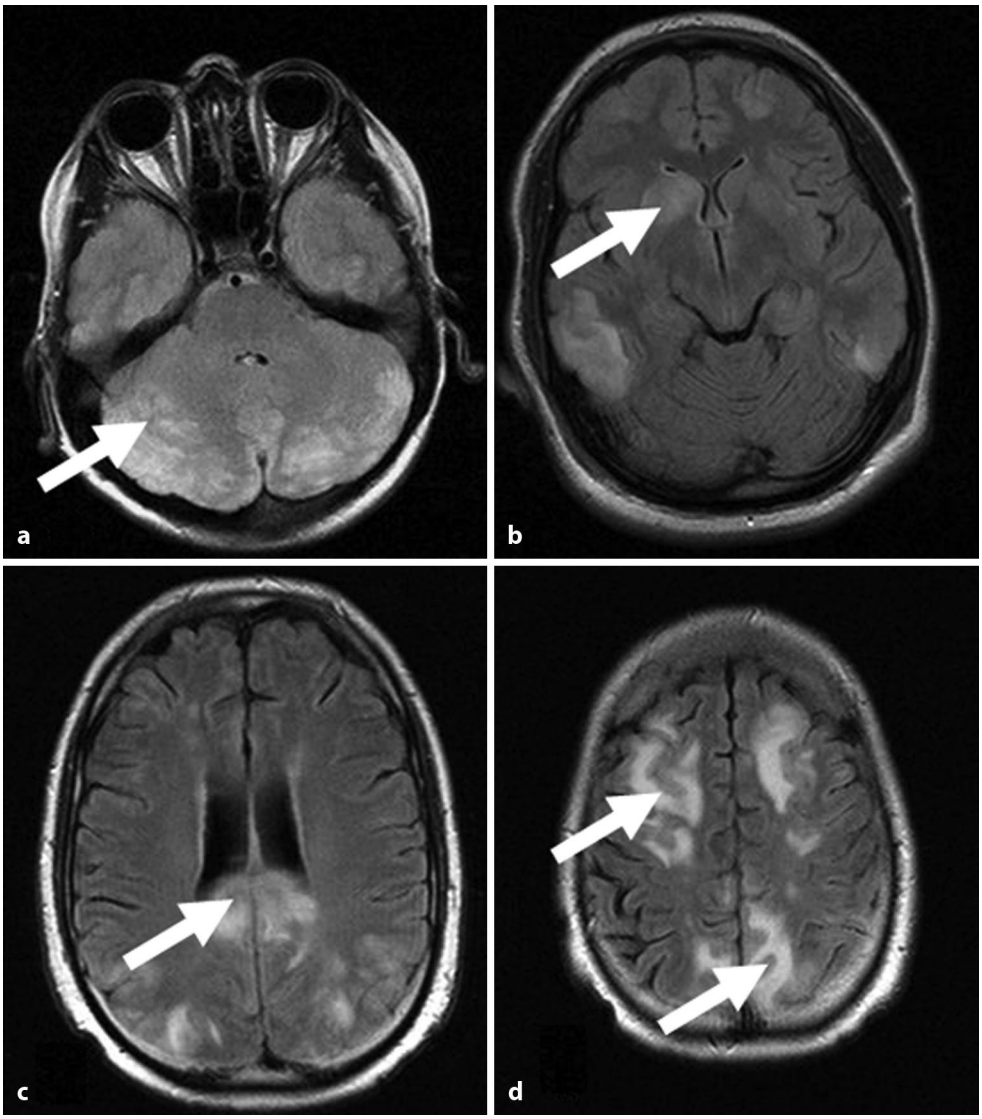

Fig. 2 Representative localizations on fluid-attenuated inversion recovery images (**a–d**, *white arrows*): mainly cerebellar (**a**), basal ganglia involvement (**b**), parieto-occipital and splenium (**c**), and fronto-parietal (**d**)

prognostic marker, as even patients with cytotoxic edema did not show conversion to infarction. It has been proposed that vasculopathy is common [32] and that an immune challenge with T-cell/endothelial activation as the trigger for vasoconstriction is often present [33]. In our study, MRA was not performed regularly, and only four patients had normal MRA findings. Thus, we are unable to comment on the frequency of vasculopathy or vasoconstriction.

Hemorrhagic changes were seen in approximately 17% of patients on T2* or SWI imaging, and subarachnoid hemorrhage was not seen, which is in keeping with a previous study [14]. A more recent study identified parenchymal bleeding in 19.4% of cases and subarachnoid hemorrhage in 6% [34]. Changes in our study were mostly subtle, and large hemorrhage was not seen. Subtle microbleeds were the only residue even after full resolution on FLAIR (Fig. 3). Thus, SWI imaging should be recommended for follow-up before stating full morphological remission.

Contrast enhancement was not present in a previous small series [35]. More recent studies reported enhancement in a variable incidence, ranging from 25% in a smaller [19] to 37.7% in a larger series of PRES [14]. Our results of 23.1% are slightly lower, but corroborate that enhancement is not a rare finding and must be expected in a subtle spot-like manner in about a quarter of patients with PRES. More diffuse and widespread enhancement was seen in two cases (Fig. 4). A single case of leptomeningeal enhancement is a finding not previously reported. This could be interpreted as leakage due to toxic effects or inflammation.

Our results on follow-up support the assumption that lesion resolution occurs in most but not all patients. Single patients with clinical and morphological persistent changes have recently been reported [36]. Three-quarters of our patients with variable predisposing factors showed full reversion, and in almost a quarter, there was marked regression. Our subanalysis of hypertensive and nonhyper-

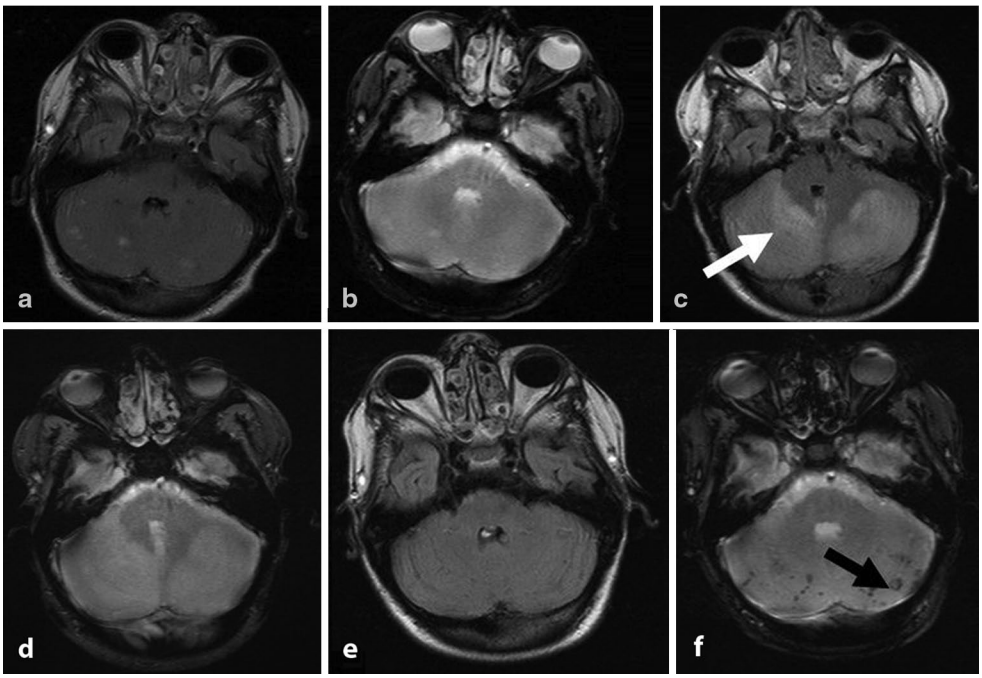

Fig. 3 Initial magnetic resonance imaging (MRI) showed spot-like hyperintensities on fluid-attenuated inversion recovery (FLAIR) (**a**) and no hemorrhage on T2* (**b**). The MRI 5 days later showed progressive extensive hyperintensity on FLAIR (**c**, *white arrow*) without hemorrhage on T2* (**d**). The follow-up 3 months later showed normalization on FLAIR (**e**), but spot-like hemorrhage on T2* (**f**, representative *white arrow*)

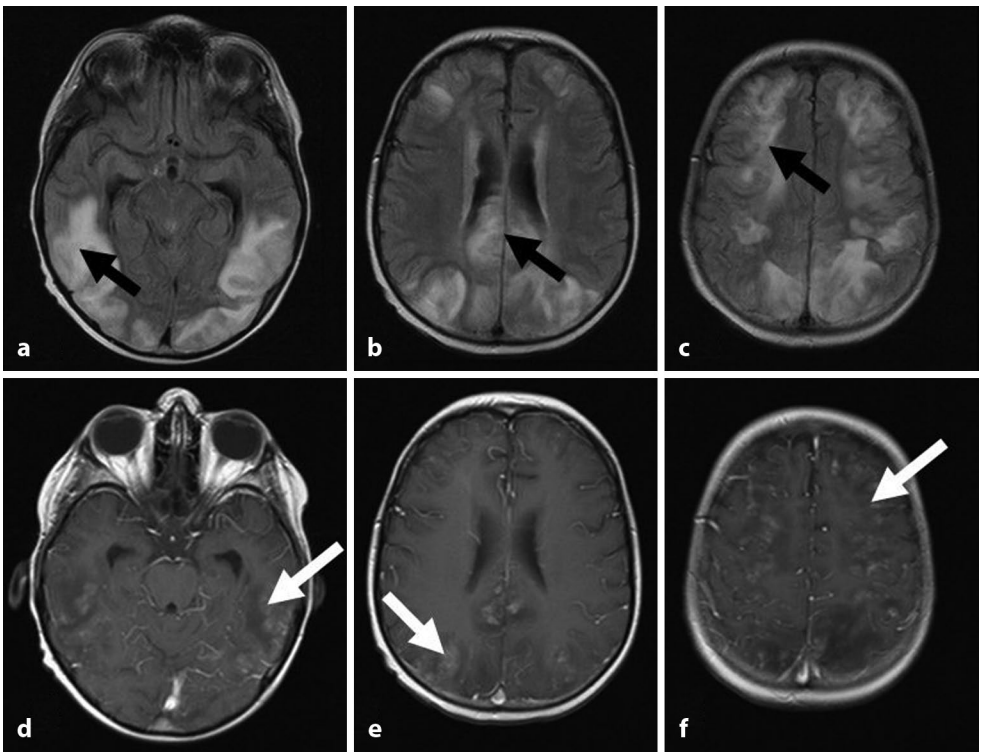

Fig. 4 Hyperintensities in the temporo-occipital (**a**), parieto-occipital and in the dorsal splenium (**b**), and fronto-parietal (**c**) regions on fluid-attenuated inversion recovery (*black arrows*). T1 after gadolinium application with diffuse patchy enhancement (**d**–**f**, *white arrows*)

tensive patients demonstrates that in our cohort, hypertension was not a prognostic indicator. Rates of reversibility were not different in both groups. Progression in the very acute phase before PRES if corrected would not be unusual. Surprisingly, one patient showed lesion expansion on repeat MRI after 2 months, most probably due to repeated toxic exposure to chemotherapy. A previous study found that reversibility was lower in deep white matter and infratentorial structures than typical cortical or subcortical ones and that reversibility was best in eclampsia [37], a finding we could not replicate. It has been postulated that the extent of edema has prognostic implications and that DWI can help predict the progression to infarction [17]. Extent of edema in our case was not a marker for infarction in those patients available for follow-up. Patients with various extent of edema showed MRI resolution to the same extent. Also in

our series, extent and patterns on DWI were not a predictor for resolution. Moreover, in patients with cytotoxic edema, there was complete resolution. This has been reported in a single case earlier [38]. This suggests that previous reports stressing the prognostic value of DWI in PRES must be regarded with caution. Cytotoxic edema in the acute phase does by no means imply conversion into infarction. This has been pointed out before in case reports [29, 39]. Our findings could potentially be skewed by the fact that in 20% of cases, follow-up was not available due to death in the further course of their underlying disease or referral to their primary hospital. Still, we consider the prognostic value of DWI in the acute phase of PRES as limited.

In patients with a suspicion of PRES, MRI is the method of choice. FLAIR, T1 before and after contrast enhancement, DWI, and SWI sequences should be performed to detect all possible changes in the acute phase and follow-up.

In sum, the present study demonstrates that the spectrum of imaging findings in PRES is wide, which has to be considered when interpreting the MRI. The term PRES implies a uniform pattern, which we could not corroborate. Almost all patients have involvement of several brain areas. Signal intensity changes and extension of lesions on FLAIR are variable without any specific pattern, and subcortical and cortical structures are almost always involved. Not only was parietal involvement at least as common as occipital, but also frontal involvement was frequent on FLAIR imaging and also pronounced on DWI, which can be heterogeneous and show normal findings or cytotoxic or vasogenic edema. Contrast enhancement must be expected in a subtle spot-like manner in about a quarter of patients with PRES. More diffuse and widespread enhancement or leptomeningeal enhancement is a rare finding.

Our findings on follow-up show that it is a dynamic process that changes individually over time. Reversibility generally takes place. Increasing lesion load was seen in one case (supplementary information Fig. 6), and new microhemorrhage in two cases, a finding not previously reported, demonstrating that the condition can progress even after the acute phase, a finding clinicians and neuroradiologists should be aware of.

We conclude that in the light of the aforementioned findings, the term RPLS or PRES does not cover all clinical and pathophysiologic aspects of this condition.

Conflict of Interest The authors declare that there are no actual or potential conflicts of interest in relation to this article.

References

1. Garg RK. Posterior leukoencephalopathy syndrome. Postgrad Med J. 2001;77:24–8.
2. Kwon S, Koo J, Lee S. Clinical spectrum of reversible posterior leukoencephalopathy syndrome. Pediatr Neurol. 2001;24:361–4.
3. Ahn KJ, Lee JW, Hahn ST, Yang DW, Kim PS, Kim HJ, Kim CC. Diffusion-weighted MRI and ADC mapping in FK506 neurotoxicity. Br J Radiol. 2003;76:916–9.
4. Gijtenbeek JM, van den Bent MJ, Vecht CJ. Cyclosporine neurotoxicity: a review. J Neurol. 1999;246:339–46.
5. Idilman R, De Maria N, Kugelmas M, Colantoni A, Van Thiel DH. Immunosuppressive drug-induced leukoencephalopathy in patients with liver transplant. Eur J Gastroenterol Hepatol. 1998;10:433–6.
6. Freise CE, Rowley H, Lake J, Hebert M, Ascher NL, Roberts JP. Similar clinical presentation of neurotoxicity following FK 506 and cyclosporine in a liver transplant recipient. Transplant Proc. 1991;23:3173–4.
7. Dicuonzo F, Salvati A, Palma M, Lefons V, Lasalandra G, De Leonardis F, Santoro N. Posterior reversible encephalopathy syndrome associated with methotrexate neurotoxicity: conventional magnetic resonance and diffusion-weighted imaging findings. J Child Neurol. 2009;24:1013–8.
8. Kastrup O, Maschke M, Wanke I, Diener HC. Posterior reversible encephalopathy syndrome due to severe hypercalcemia. J Neurol. 2002;249:1563–6.
9. Kastrup O, Diener HC. Granulocyte-stimulating factor filgrastim and molgramostim induced recurring encephalopathy and focal status epilepticus. J Neurol. 1997;244:274–5.
10. Kastrup O, Diener HC. TNF-antagonist etanercept induced reversible posterior leukoencephalopathy syndrome. J Neurol. 2008;255:452–3.
11. Hinchey J, Chaves C, Appignani B, Breen J, Pao L, Wang A, Pessin MS, Lamy C, Mas JL, Caplan LR. A reversible posterior leukoencephalopathy syndrome. N Engl J Med. 1996;334:494–500.
12. Ni J, Zhou LX, Hao HL, Liu Q, Yao M, Li ML, Peng B, Cui LY. The clinical and radiological spectrum of posterior reversible encephalopathy syndrome: a retrospective series of 24 patients. J Neuroimaging. 2011;21:219–24.
13. Bartynski WS, Boardman JF. Distinct imaging patterns and lesion distribution in posterior reversible encephalopathy syndrome. AJNR Am J Neuroradiol. 2007;28:1320–7.
14. McKinney AM, Short J, Truwit CL, McKinney ZJ, Kozak OS, SantaCruz KS, Teksam M. Posterior reversible encephalopathy syndrome: incidence of atypical regions of involvement and imaging findings. AJR Am J Roentgenol. 2007;189:904–12.
15. Psychogios MN, Schramm P, Knauth M. [Reversible encephalopathy syndrome, RES or PRES: a case with more W (watershed) than P (posterior)!]. Rofo. 2010;182:76–9.
16. Kinoshita T, Moritani T, Shrier DA, Hiwatashi A, Wang HZ, Numaguchi Y, Westesson PL. Diffusion-weighted MR imaging of posterior reversible leukoencephalopathy syndrome: a pictorial essay. Clin Imaging. 2003;27:307–15.
17. Covarrubias DJ, Luetmer PH, Campeau NG. Posterior reversible encephalopathy syndrome: prognostic utility of quantitative diffusion-weighted MR images. AJNR Am J Neuroradiol. 2002;23:1038–48.
18. Bhagavati S, Choi J. Atypical cases of posterior reversible encephalopathy syndrome. Clinical and MRI features. Cerebrovasc Dis. 2008;26:564–6.
19. Donmez FY, Basaran C, Kayahan Ulu EM, Yildirim M, Coskun M. MRI features of posterior reversible encephalopathy syndrome in 33 patients. J Neuroimaging. 2010;20:22–8.
20. Sheth RD, Riggs JE, Bodenstenier JB, Gutierrez AR, Ketonen LM, Ortiz OA. Parietal occipital edema in hypertensive encephalopathy: a pathogenic mechanism. Eur Neurol. 1996;36:25–8.
21. Ay H, Buonanno FS, Schaefer PW, Le DA, Wang B, Gonzalez RG, Koroshetz WJ. Posterior leukoencephalopathy without se-

vere hypertension: utility of diffusion-weighted MRI. Neurology. 1998;51:1369–76.
22. Casey SO, Sampaio RC, Michel E, Truwit CL. Posterior reversible encephalopathy syndrome: utility of fluid-attenuated inversion recovery MR imaging in the detection of cortical and subcortical lesions. AJNR Am J Neuroradiol. 2000;21:1199–206.
23. Lamy C, Oppenheim C, Meder JF, Mas JL. Neuroimaging in posterior reversible encephalopathy syndrome. J Neuroimaging. 2004;14:89–96.
24. Striano P, Striano S, Tortora F, De Robertis E, Palumbo D, Elefante A, Servillo G. Clinical spectrum and critical care management of posterior reversible encephalopathy syndrome (PRES). Med Sci Monit. 2005;11:CR549–53.
25. Weingarten K, Barbut D, Filippi C, Zimmerman RD. Acute hypertensive encephalopathy: findings on spin-echo and gradient-echo MR imaging. AJR Am J Roentgenol. 1994;162:665–70.
26. Doelken M, Lanz S, Rennert J, Alibek S, Richter G, Doerfler A. Differentiation of cytotoxic and vasogenic edema in a patient with reversible posterior leukoencephalopathy syndrome using diffusion-weighted MRI. Diagn Interv Radiol. 2007;13:125–8.
27. Coughlin WF, McMurdo SK, Reeves T. MR imaging of postpartum cortical blindness. J Comput Assist Tomogr. 1989;13:572–6.
28. Trommer BL, Homer D, Mikhael MA. Cerebral vasospasm and eclampsia. Stroke. 1988;19:326–9.
29. Benziada-Boudour A, Schmitt E, Kremer S, Foscolo S, Riviere AS, Tisserand M, Boudour A, Bracard S. Posterior reversible encephalopathy syndrome: a case of unusual diffusion-weighted MR images. J Neuroradiol. 2009;36:102–5.
30. Schneider JP, Krohmer S, Gunther A, Zimmer C. [Cerebral lesions in acute arterial hypertension: the characteristic MRI in hypertensive encephalopathy]. Rofo. 2006;178:618–26.
31. Provenzale JM, Petrella JR, Cruz LC Jr, Wong JC, Engelter S, Barboriak DP. Quantitative assessment of diffusion abnormalities in posterior reversible encephalopathy syndrome. AJNR Am J Neuroradiol. 2001;22:1455–61.
32. Bartynski WS, Boardman JF. Catheter angiography, MR angiography, and MR perfusion in posterior reversible encephalopathy syndrome. AJNR Am J Neuroradiol. 2008;29:447–55.
33. Bartynski WS. Posterior reversible encephalopathy syndrome, part 2: controversies surrounding pathophysiology of vasogenic edema. AJNR Am J Neuroradiol. 2008;29:1043–9.
34. McKinney AM, Sarikaya B, Gustafson C, Truwit CL. Detection of microhemorrhage in posterior reversible encephalopathy syndrome using susceptibility-weighted imaging. AJNR Am J Neuroradiol. 2012;33:896–903.
35. Ugurel MS, Hayakawa M. Implications of post-gadolinium MRI results in 13 cases with posterior reversible encephalopathy syndrome. Eur J Radiol. 2005;53:441–9.
36. Iwama M, Takahashi H, Takagi R, Hiraoka M. Permanent bilateral cortical blindness due to reversible posterior leukoencephalopathy syndrome. J Nippon Med Sch. 2011;78:184–8.
37. Pande AR, Ando K, Ishikura R, Nagami Y, Takada Y, Wada A, Watanabe Y, Miki Y, Uchino A, Nakao N. Clinicoradiological factors influencing the reversibility of posterior reversible encephalopathy syndrome: a multicenter study. Radiat Med. 2006;24:659–68.
38. Ulrich K, Troscher-Weber R, Tomandl BF, Neundorfer B, Reinhardt F. Posterior reversible encephalopathy in eclampsia: diffusion-weighted imaging and apparent diffusion coefficient-mapping as prognostic tools? Eur J Neurol. 2006;13:309–10.
39. Yilmaz S, Gokben S, Arikan C, Calli C, Serdaroglu G. Reversibility of cytotoxic edema in tacrolimus leukoencephalopathy. Pediatr Neurol. 2010;43:359–62.